RSC Advances

PAPER

Check for updates

Synthesis and conductive performance of polyoxometalate acid salt gel electrolytes

Limei Ai,[a] Zeqing Wang,[a] Fengwei He[a] and Qingyin Wu ⓘ *[ab]

Two vanadium-substituted polyoxometalate acid salt gel electrolytes, $[PyPS]_3H_4SiW_9V_3O_{40}$ and $[PyPS]_5H_2SiW_9V_3O_{40}$, have been synthesized using a 1-(3-sulfonic group) propylpyridine (PyPS) and a Keggin vanadium-substituted heteropoly acid $H_7SiW_9V_3O_{40}$ through an ionic self-assembly method, and adjusting the ratio of cation and anion. A substitution effect of the acid salt gel electrolytes has been investigated. Interestingly, when protons of the polyoxometalate acid salt gel electrolytes are substituted, both the conductivity and the phase transformation temperature increase. The fastest conductivity of these gel electrolytes was as high as 2.57×10^{-2} S cm^{-1} at 110 °C.

1. Introduction

Heteropoly acids (HPAs) or polyoxometalates (POMs) are a type of metal oxide cluster. It is formed by inorganic metal oxygen cluster anions that means a variety of structures and characteristics can be obtained.[1,2] Therefore, polyoxometalate-based compounds show interesting electronic, magnetic, redox, medicinal and photonic properties.[3–7] In particular, detailed research into conduction in these compounds will inspire the development of fuel cells and electrochemical electrolytes based on POMs.[8–12] However, the machinability of POMs is poor, and the conductivity is highly related to the amount of water molecules in the POM structure. Thus, the conductivity will be decreased at high temperature.[13]

Ionic liquids (ILs) are a type of excellent molten salt since it remains in the liquid phase at room temperature. The preparation of the ionic liquids based on relatively large organic cations and inorganic anions through ionic self-assembly. Ionic liquids have many excellent properties in range of physicochemical, such as thermal stability and electrochemical applications.[14–16] Many kinds of novel ionic liquids have been synthesized by different cations and anions with ionic self-assembly effect.[17,18]

Recently, many researcher found that the combination of the physical properties of POMs with those of IL salts generated a "chimera", which exhibits a liquid-like property.[19] These materials show a quasi-solid state at room temperature, and it is changed to a liquid state when being heated to about 100 °C.[20] Consequently, the quasi-solid state materials exhibit higher ionic conductivity than that of other solid conductors and have

advantages over both a liquid electrolyte and a solid state electrolyte, which makes this new class of materials potential candidates for electrolyte in advanced electrochemical devices.[21–25] However, many researcher focus on the normal salts of the polyoxometalates ionic liquids (POM-ILs) and there are few articles reported about the acid salts (POM-ASs) of POM-ILs.

Generally, Keggin-type heteropoly acids have many special characteristics such as stable structure, simple preparation method and high yield. Thus, we chose a Keggin-type vanadium-substituted HPA ($H_7SiW_9V_3O_{40}$) and the pyridine class with sulfonic group functional compound, 1-(3-sulfonic group) propylpyridine (PyPS) to synthesize a series of POM-based ionic liquids through the ionic self-assembly method. The phase transformation, structure and conductive performance of two POM-ASs compounds were characterized.

2. Experimental section

2.1 Instrument and reagent

Elemental analysis was determined by inductively coupled plasma (ICP-MS) analysis on a Shimadzu V-1012 ICP-MS spectrometer. Infrared (IR) spectrum was conducted on a NICOLET NEXUS 470 FT/IR spectrometer during the wavenumber range 400–4000 cm^{-1} using KBr pellet. X-ray powder diffraction (XRD) pattern was conducted on a BRUKER D8 ADVANCE X-ray diffractometer using a Cu tube at the conditions: at 40 kV and 40 mA in the range of $2\theta = 4–40°$ at a rate of $0.02° \cdot s^{-1}$. The thermal stability of these samples was reported on a SHIMADZU thermal analyzer. Conductivity was measured through a DDS-11A conductivity meter using a Shanghai DJS-1 and DJS-10 electrode. The UV absorption spectra were monitored by a Specord TU-1901 UV-vis spectrophotometer.

All the chemicals were of analytical grade and used without further purification.

[a]School of Biomedical and Chemical Engineering, Liaoning Institute of Science and Technology, Benxi 117004, Liaoning, P. R. China. E-mail: qywu@lnist.edu.cn; qywu@zju.edu.cn

[b]Department of Chemistry, Zhejiang University, Hangzhou, 310027, P. R. China

This journal is © The Royal Society of Chemistry 2018

2.2. Synthesis of the POM-ASs

1-(3-Sulfonic group) propylpyridine (PyPS) was synthesized according to the literature.[23] $H_7SiW_9V_3O_{40}$ was synthesized as follow, $Na_{10}[\alpha\text{-}SiW_9O_{34}]$ was synthesized by a method according to recent literature. A 10 mL aqueous solution of sodium metavanadate (1.71 g $NaVO_3$) was added to a 30 mL aqueous solution of $Na_{10}[\alpha\text{-}SiW_9O_{34}]$ (10 g $Na_{10}[\alpha\text{-}SiW_9O_{34}]$). The mixture was adjusted to pH = 1.5. And then, the mixture was added into the H^+ type cation exchange resin column at room temperature, until the pH of the mixture is less than 1. The mixture was dried at 40 °C and a orange power was obtained.

The pre-synthesized PyPS and $H_7SiW_9V_3O_{40}$ were taken in 3 : 1 and 5 : 1 mole ratios to give one mole of $[PyPS]_3H_4SiW_9V_3O_{40}$ and $[PyPS]_5H_2SiW_9V_3O_{40}$. PyPS was added into an aqueous solution of $H_7SiW_9V_3O_{40}$. The mixture was reacted under ultrasound for 10 minutes at room temperature, and then collected bottom layer liquid. The liquid evaporated at room temperature and then the product as oily gel-type was obtained.

3. Results and discussion

The detail IR spectra of the compounds at 1100–700 cm^{-1} is shown in the Fig. 1 and Table 1. As shown in the Fig. 1 and Table 1, we can clearly find that these feature frequencise, all compounds, fall in the stretching sequence of $\nu as(Si–O_a)$, $\nu as(M–O_d)$, $\nu as(M–O_b–M)$ and $\nu as(M–O_c–M)$, (M = W, V), which is referred to POM character bands at 1100–700 cm^{-1}. We also find the shift of characteristic peaks of POM-ASs in the Fig. 1 and Table 1 when compared with POM. This phenomenon can be explained by the vibrations frequency change result in the
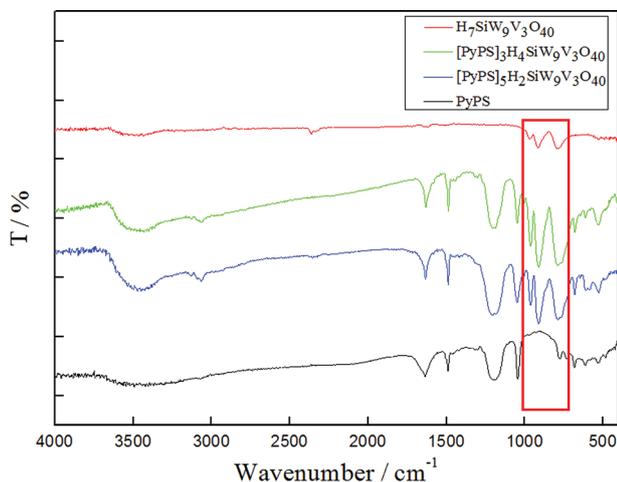
influence of the anion–anion interactions among polyoxoanions.[26,27] In spite of the shift of characteristic peaks of POM-ASs, the peaks still exists, which can find at a red zone in the Fig. 1. The result infer that these compounds still maintain POM structure without decomposition, when PyPS added.

The POM in non-reduced state is generally characterized by charge transfer bands of oxygen-to-metal, which can be observed by UV-vis spectrophotometer in the UV region below 400 nm. The UV absorption spectrum of the compounds is shown in the Fig. 2. As shown in the Fig. 2, we can find that the absorption bands of $H_7SiW_9V_3O_{40}$, $[PyPS]_3H_4SiW_9V_3O_{40}$ and $[PyPS]_5H_2SiW_9V_3O_{40}$ appear at about 260 nm, 259 nm, 260 nm, respectively. The absorption spectrum of POM-ILs display a moderately intense peak nearly 259 nm (O–M) and the peak is blue-shifted from 260 nm which is referred to the pure POM.[28] This phenomenon can provide an evidence for intermolecular interactions between PyPS cations and Keggin-type anion units.

Wide-angle XRD patterns of POM and POM-ASs are shown in the Fig. 4. The intensity is very strong peaks in the large region of the XRD patterns of $H_7SiW_9V_3O_{40}$. The Keggin-type of the polyoxometalates which exhibited typical peaks in the range of $2\theta = 7–11°$ in the XRD patterns was found. From that phenomenon, it is clear that the POM compound was successfully prepared. Furthermore, we also found a broad diffraction peaks in the region of $2\theta = 20–35°$ of POM-ASs, which indicates the distinction between the POM-ASs and their parent HPA.[29] $[PyPS]_3H_4SiW_9V_3O_{40}$ and $[PyPS]_5H_2SiW_9V_3O_{40}$ present similar XRD pattern. This phenomenon infers that the parent HPA is changes into amorphous structure after the acidic protons (PyPS) were added.

These POM-ASs exhibit a characteristic of reversible gel–liquid phase transformation. Fig. 5 shows the POM-ASs phase transform between gel state and liquid state at 100 °C. Since the weak connection among PyPS cation, POM anion and protons, the gel state of POM-ASs exhibit amorphous state, which can be proved by XRD patterns, and the schematic is shown in Fig. 3.

The variation of the conductivity of these compounds can be observed with heating. The results of variation of conductivity show in the Fig. 6. As shown in the Fig. 6, it can find that there is
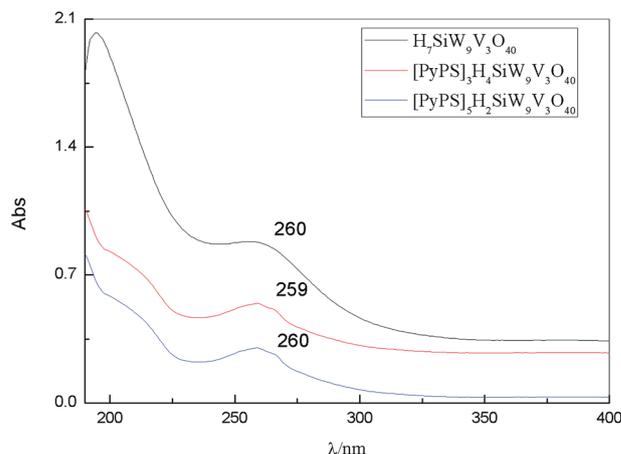

Fig. 1 IR spectra of the compounds.

Table 1 The detail IR spectra of compounds at 1100–700 cm^{-1}

Vibrations/cm^{-1}	SiW_9V_3	$[PyPS]_3H_4SiW_9V_3$	$[PyPS]_5H_2SiW_9V_3$
M–O$_d$ stretching	970	960	962
Si–O$_a$ stretching	914	911	908
M–O$_c$–M stretching	785	790	788

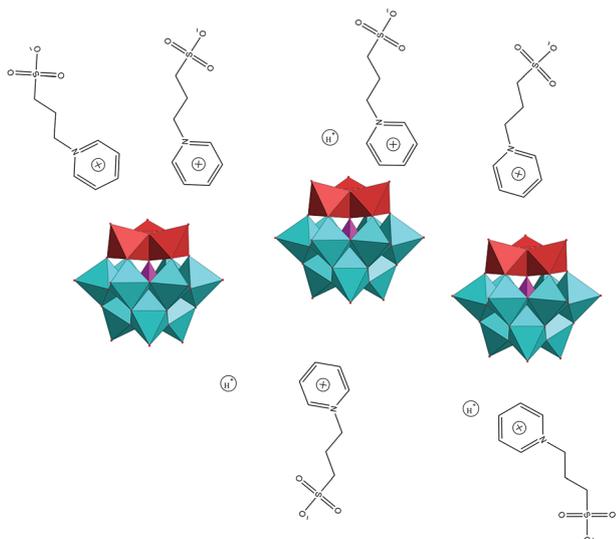Fig. 2 The UV absorption spectra of the HPA and POM-ASs.

Fig. 3 Schematic illustration of potential weak connections in these compounds among PyPS, protons and POM anion.

a broad endothermic peak at about 85 °C for $[PyPS]_3H_4SiW_9V_3O_{40}$ and at about 70 °C for $[PyPS]_5H_2SiW_9V_3O_{40}$. That phenomenon can be attributed to a phase transformation from a solid gel phase to an isotropic liquid phase.[30] It can also find that the conductivity of these compounds increase with heating, especially at the time that these compounds at the temperature
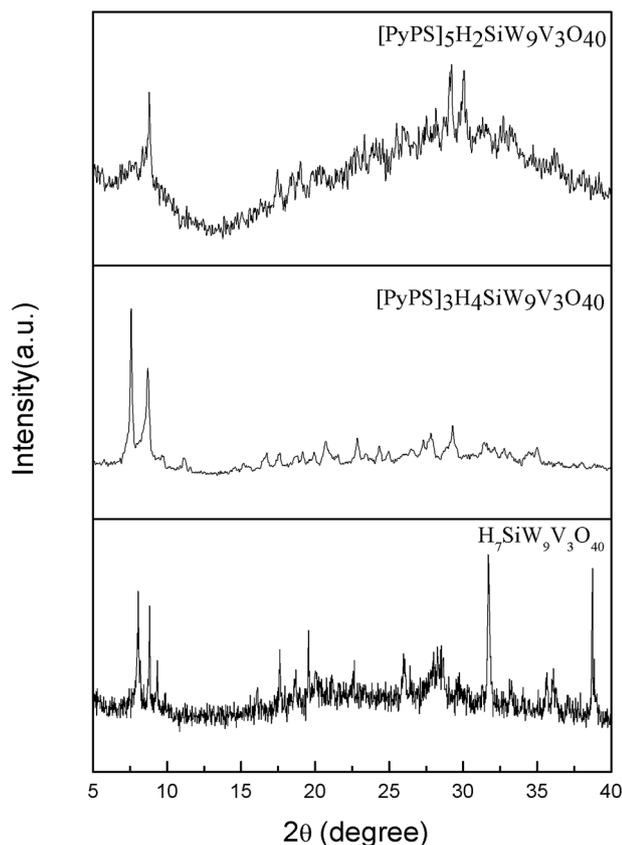

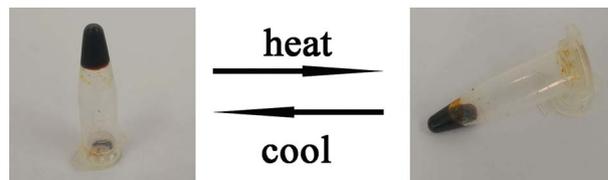**Fig. 4** Wide-angle XRD patterns of the HPA and POM-ASs.

Fig. 5 Photographs of the $[PyPS]_3H_4SiW_9V_3O_{40}$ reversible gel–liquid phase transformation at room temperature and 100 °C.

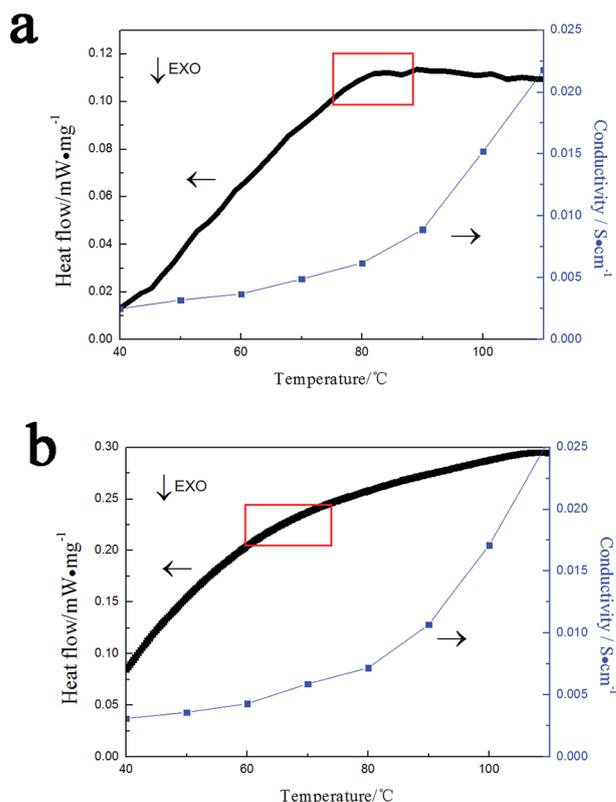**Fig. 6** Conductivity–temperature and heat flow curves of (a) $[PyPS]_3H_4SiW_9V_3O_{40}$ and (b) $[PyPS]_5H_2SiW_9V_3O_{40}$.

of phase transformation from gel to liquid, the phenomenon of increasing conductivity is obvious. Concretely, at 110 °C the conductivity of $[PyPS]_3H_4SiW_9V_3O_{40}$ and $[PyPS]_5H_2SiW_9V_3O_{40}$ is 2.57×10^{-2} S cm^{-1} and 2.18×10^{-2} S cm^{-1}, respectively. The phenomenon can be resulted in an increase in the migration of particles in the compound.

Fig. 7 shows conductivity of different amount of PyPS substitution at different temperature. Obviously, when the number of protons in the compound increase, the conductivity of these compounds enhance accordingly. This phenomenon can be explained as that the protons in the compounds migrate much faster than PyPS. Thus it is found that the higher conductivity can result from more protons in the compound. Additionally, when many protons have substituted the PyPS, the conductivity of the compounds also increase. So it is infer that more protons in the compounds will result in higher conductivity. Furthermore, this result also can be confirmed by conductive activation energy.[31,32]
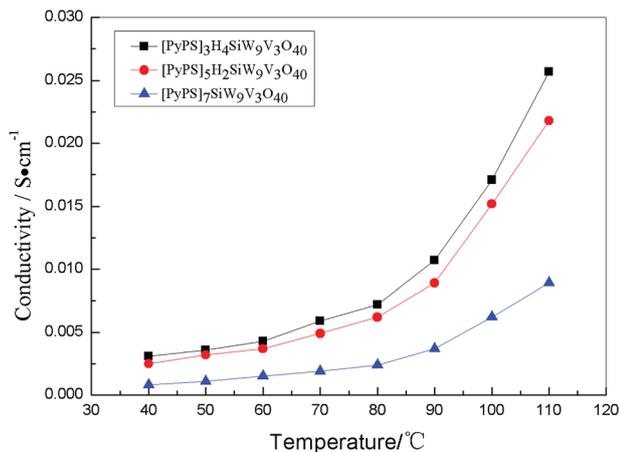
Fig. 7 Conductivity–temperature plots of $[PyPS]_3H_4SiW_9V_3O_{40}$, $[PyPS]_5H_2SiW_9V_3O_{40}$ and $[PyPS]_7SiW_9V_3O_{40}$.
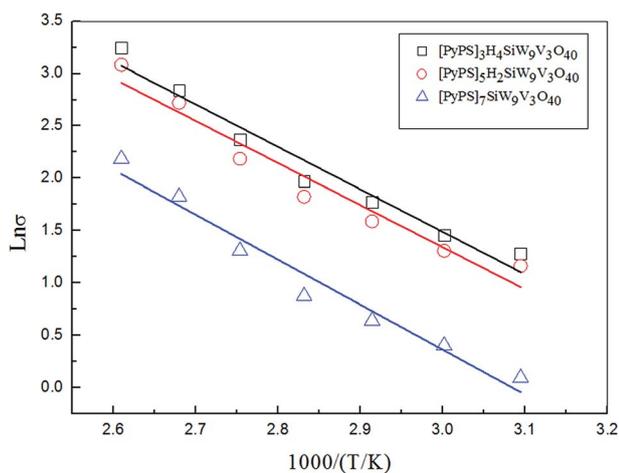
Fig. 8 The conductive Arrhenius plots of $[PyPS]_3H_4SiW_9V_3O_{40}$, $[PyPS]_5H_2SiW_9V_3O_{40}$ and $[PyPS]_7SiW_9V_3O_{40}$ at the same condition.

The conductive activation energy E_a can be evaluated as follow

$$\sigma = \sigma_0 \exp\left(\frac{-E_a}{RT}\right)$$

where σ is conductive, σ_0 is the pre-exponential factor, E_a is the conductive activation energy, R is the gas constant and T is the absolute temperature. Fig. 8 shows the conductive Arrhenius plots of $[PyPS]_3H_4SiW_9V_3O_{40}$, $[PyPS]_5H_2SiW_9V_3O_{40}$ and $[PyPS]_7$-$SiW_9V_3O_{40}$ at the same condition. The values of E_a of these compounds can be obtained by linear fit and the values of E_a for $[PyPS]_3H_4SiW_9V_3O_{40}$, $[PyPS]_5H_2SiW_9V_3O_{40}$ and $[PyPS]_7SiW_9V_3$-O_{40} is 33.4 kJ mol^{-1}, 33.7 kJ mol^{-1} and 35.7 kJ mol^{-1}, respectively. In this case, it is found that number of protons have an obvious influence on conductivity of the compounds.

4. Conclusions

In this paper, we have reported two vanadium-substituted polyoxometalate acid salts gel electrolytes, $[PyPS]_3H_4SiW_9V_3O_{40}$

and $[PyPS]_5H_2SiW_9V_3O_{40}$. These electrolytes exhibit reversible gel–liquid phase transformation. A relationship among the conductivity, substituted protons and temperature can be observed by heat flow and conductivity plots. The results indicate that the conductivity and phase transformation temperature improve with increasing the number of protons in the compounds. Thus these materials maybe provide both liquid state electrolytes and solid state electrolytes for supercapacitors.

Conflicts of interest

There are no conflicts to declare.

Acknowledgements

References

1 M. Shiddiq, D. Komijani, D. Yan, A. Gaitaariño, E. Coronado and S. Hill, *Nature*, 2016, **531**, 348–351.

2 Z. Chen, W. B. Bu, D. L. Ni, C. J. Zuo, C. Chao, Q. Li, L. L. Zhang, W. Zheng and J. L. Shi, *J. Am. Chem. Soc.*, 2016, **138**, 8156–8164.

3 A. Rubinstein, P. Jiménezlozanao, J. J. Carbó, J. M. Poblet and R. Neumann, *J. Am. Chem. Soc.*, 2014, **136**, 10941–10948.

4 T. Yoshida, T. Murayama, N. Sakaguchi, M. Okumura, T. Ishida and M. Haruta, *Angew. Chem., Int. Ed.*, 2018, **57**, 1523–1527.

5 J. J. Chen, M. D. Symes, S. C. Fan, M. S. Zheng, H. N. Miras, Q. F. Dong and L. Cronin, *Adv. Mater.*, 2017, **27**, 4649–4654.

6 Y. W. Liu, S. M. Liu, X. Y. Lai, J. Miao, D. F. He, N. Li, F. Luo, Z. Shi and S. X. Liu, *Adv. Funct. Mater.*, 2015, **25**, 4480–4485.

7 X. Tong, N. Q. Tian, W. Wu, W. M Zhu, Q. Y. Wu, F. H. Cao, W. F. Yan and A. B. Yaroslavtsev, *J. Phys. Chem. C*, 2013, **117**, 3258–3263.

8 J. J. Chen, J. C. Ye, X. G. Zhang, M. D. Symes, S. C. Fan, D. L. Long, M. S. Zheng, D. Y. Wu, L. Cronin and Q. F. Dong, *Adv. Energy Mater.*, 2018, **8**, 1701021.

9 M. H. Yang, B. G. Choi, S. C. Jung, Y. K. Han, Y. S. Huh and S. B. Lee, *Adv. Funct. Mater.*, 2015, **24**, 7301–7309.

10 H. Gao, A. Virya and K. Lian, *J. Mater. Chem. A*, 2015, **3**, 21511–21517.

11 M. Tountas, Y. Topal, A. Verykios, A. Soultati, A. Kaltzoglou, T. A. Papadopoulos, F. Auras, K. Seintis, M. Fakis and L. C. Palilis, *J. Mater. Chem. C*, 2018, **6**, 1459–1469.

12 X. F. Wu, W. Wu, Q. Y. Wu and W. F. Yan, *Langmuir*, 2017, **33**, 4242–4249.

13 W. B. Kim, T. Voitl, G. J. Rodriguezrivera and J. A. Dumesic, *Science*, 2004, **305**, 1280–1283.

14 W. L. Zhou, J. Peng, Z. Y. Zhang, Z. Y. Shi, S. U. Khan and H. S. Liu, *RSC Adv.*, 2015, **5**, 35753–35759.

15 E. Rafiee, S. Eavani, X. Cai, X. F. Wu, R. S. Anaredy and S. K. Shaw, *RSC Adv.*, 2016, **6**, 46433–46466.

16 R. Hayes, G. G. Warr and R. Atkin, *Chem. Rev.*, 2015, **115**, 6357–6426.

17 E. Elfassy, Y. Mastai, D. Pontoni and M. Deutsch, *Langmuir*, 2016, **32**, 3164–3173.

18 Q. Y. Wu, X. Tong and X. F. Wu, *J. Xuzhou Inst. Technol., Nat. Sci. Ed.*, 2011, **26**, 1–8.

19 J. Azizullah, M. Al-Rashida, A. Haider, U. Kortz, S. A. Joshi and J. Iqbal, *ChemistrySelect*, 2018, **3**, 1472–1479.

20 A. B. Bourlinos, K. Raman, R. Herrera, Q. Zhang, L. A. Archer and E. P. Giannelis, *J. Am. Chem. Soc.*, 2004, **126**, 15358–15359.

21 S. Akbani, M. T. Hamed Mosavian, F. Moosavi and A. Ahmadpour, *RSC Adv.*, 2017, **7**, 44537–44546.

22 A. R. Neale, C. Schütter, P. Wilde, P. Goodrich, C. Hardacre, S. Passerini, A. Balducci and J. Jacquemin, *J. Chem. Eng. Data*, 2017, **62**, 376–390.

23 Y. Leng, J. Wang, D. R. Zhu, X. Q. Ren, H. Q. Ge and L. Shen, *Angew. Chem., Int. Ed.*, 2010, **48**, 168–171.

24 X. F. Wu, X. H. Zhou, Q. Y. Wu and W. F. Yan, *New J. Chem.*, 2016, **40**, 7923–7927.

25 Y. Y. Li, X. F. Wu, Q. Y. Wu, H. Ding and W. F. Yan, *Dalton Trans.*, 2014, **43**, 13591–13595.

26 Z. K. Zhao, Y. T. Dai, T. Bao, R. Z. Li and G. R. Wang, *J. Catal.*, 2012, **288**, 44–53.

27 T. P Huang, N. Q. Tian, Q. Y. Wu and W. F. Yan, *Soft Matter*, 2015, **11**, 4481–4486.

28 X. F. Wu, X. Tong, Q. Y. Wu, H. Ding and W. F. Yan, *J. Mater. Chem. A*, 2014, **2**, 5780–5784.

29 Z. R. Xie, Q. Y. Wu and L. M. Ai, *Funct. Mater. Lett.*, 2018, **11**, 1850059.

30 T. L. Greaves and C. J. Drummond, *Chem. Rev.*, 2008, **108**, 206–237.

31 M. A. Hickner, H. Ghassemi, S. K. Yu, B. R. Einsla and J. E. Mcgrath, *Chem. Rev.*, 2004, **104**, 4587–4611.

32 Z. R. Xie, H. Wu, Q. Y. Wu and L. M. Ai, *RSC Adv.*, 2018, **8**, 13984–13988.